P-1761

Soft Computing Approach for Rotor Fault Detection in Three Phase Induction Motor

A Project Report

Submitted by

A. Anu - Reg. No. 71204415001

in partial fulfillment for the award of the degree
of

Master of Engineering
in
Power Electronics and Drives

DEPARTMENT OF ELECTRICAL & ELECTRONICS ENGINEERING

KUMARAGURU COLLEGE OF TECHNOLOGY
COIMBATORE – 641 006

ANNA UNIVERSITY:: CHENNAI 600 025

JUNE 2006

THIS CERTIFIES THAT

Prof./Dr./Mr./Ms. A. Anu
of Kumaraguru College of Technology
Coimbatore has participated in the SECOND NATIONAL CONFERENCE on "CUTTING EDGE TECHNOLOGIES IN POWER CONVERSION AND INDUSTRIAL DRIVES", PCID-2006 held on 24-25, March 2006 and presented a paper titled "Soft Computing Approach for Rotor Fault Detection in Three Phase Induction Motor" in the session Power Electronics of the conference.

CONVENOR PCID-2006 DEAN EEE PRINCIPAL

ANNA UNIVERSITY::CHENNAI 600 025

BONAFIDE CERTIFICATE

Certified that this project report entitled **"Soft Computing Approach for Rotor Fault Detection in Three Phase Induction Motor"** is the bonafide work of

Ms. A. Anu - Register No. 71204415001

Who carried out the project work under my supervision.

Signature of the Head of the Department
Prof K. Regupathy Subramanian

Signature of the Supervisor
Prof. V.Duraisamy

Internal Examiner

External Examiner 30/6/06

DEPARTMENT OF ELECTRICAL & ELECTRONICS ENGINEERING

KUMARAGURU COLLEGE OF TECHNOLOGY
COIMBATORE 641 006

ABSTRACT

Induction motors are widely used in industries. They are exposed to variety operating and atmospheric conditions. These conditions coupled with natural aging, causes the incipient fault in stator and rotor. Nearly 10% of the failures occur on the rotor. Majority of rotor related faults in the induction motors are due to broken bars and end rings. Faults involving several broken bars yield asymmetrical operation of induction machine. Once a bar breaks, the condition of the neighbouring bars also deteriorates progressively due to increased stresses. To prevent such a cumulative destructive process, the problem should be detected early. A simple technique for rotor fault detection based on stator current spectrum analysis is developed in this report.

In order to have intelligent fault detection, artificial neural network and fuzzy logic are used. This scheme does not require mathematical model of the motor. Also, in this report the fuzzy membership function is optimized using genetic algorithm. Since this scheme detects faults at an earlier stage, the maintenance can be carried in organized manner reducing downtime and repairing cost.

ஆய்வு சுருக்கம்

பெரும்பான்மையான மும்முனை இன்டக்சன் மோட்டார்கள், சிலவற்றால் பழுது அடைகின்றன. முக்கிமான காரணங்கள் உடைந்த சட்டங்கள், இறுதி வளையங்கள். உடைந்த சட்டங்கள் இன்டக்சன் மோட்டார்ரை சமச்சீர் இல்லா நிலையில் வைக்கின்றன. ஒருமுறை ஒரு சட்டம் உடைந்தால், தொடர் அழுத்தத்தினால் பக்கத்து சட்டங்களைச் சீர்கேடு அடையச் செய்கின்றது. இம்மாதிரியான தொடர் அழிவுச் செயலைக் கட்டுப்படுத்த இதன் பழுதை முன் கூட்டியே கண்டுபிடிக்க வேண்டும். ஒரு எளிய மின்னோட்ட நிறமாலை பகுத்தாய்தல் மூலம் ரோட்டர் பழுதை இத்திட்டம் கண்டுபிடிக்கின்றது.

இத்திட்டம் செயற்கை நியூரல் வளைப்பின்னல் மற்றும் பஸ்லி தத்துவத்தைப் பயன்படுத்தி மிக்க பயன்பாடுடையதாக உருவாக்கப்படுகின்றது. மேலும் இத்திட்டம் பஸ்லி உருப்பு சமன்பாட்டினை மரபியல் விதியைப் பயன்படுத்தி மிகவும் பயன்தக்கதாக உருவாக்கப்படுகின்றது. இத்திட்டத்தினால் இயந்திரங்களின் உதிரிபாகங்களின் பழுதை முன்கூட்டியே அறிந்து மாற்றுவதால் இயந்திரங்களின் செயல்திறன் அதிகரிப்பது மட்டுமின்றி அதன் பழுது பார்க்கும் செலவும் குறைக்கப்படுகின்றது.

ACKNOWLEDGEMENT

"A journey of thousand miles starts with a single step"

The pillar behind this single step who was instrumental in choosing and getting on with this project with invaluable guidance, moral support and encouragement is my guide **Prof.V.Duraisamy,** Assistant Professor and **Mrs.D.Somasundareswari,** Senior Lecturer, Department of Electrical and Electronics Engineering, Kumaraguru College of Technology. I am highly indebted to them for having helped me a great extent by providing fruitful suggestions for improvement.

I take this opportunity to express my sincere thanks to my course tutor **Prof.K.Regupathy Subramanian,** Head of Department, Electrical and Electronics Engineering. Kumaraguru College of Technology for his moral support and encouragement during the entire course.

I extent thanks to all faculty members in Electrical and Electronics Engineering Department, my family members and friends who provided immense encouragement and support for the completion of this project.

I thank the almighty god without whose grace this work would not have come true. I consider it as privilege to extend a few words of gratitude and respect to all those who guided and inspired me in successful completion of this project.

- A.ANU

CONTENTS

LIST OF TABLES

LIST OF FIGURES

LIST OF SYMBOLS AND ABBREVIATION

γ	-	Momentum Factor
s	-	Slip
f	-	Supply Frequency
A_1	-	Amplitude at (1-2s)f Frequency
A_2	-	Amplitude at (1+2s)f Frequency
IM	-	Induction Motor
MMF	-	Magneto Motive Force
EMF	-	Electro Motive Force
FFT	-	Fast Fourier Transform
LMS	-	Least Mean Square
FLC	-	Fuzzy Logic Controller
GA	-	Genetic Algorithm

CHAPTER 1
INTRODUCTION

The simple, robust design and construction of ac induction motors have encouraged their successful application in industry for many years. However, these motors are required to operate in highly corrosive and dusty environments. These factors coupled with the natural aging process of any motor make the motor subject to faults. These faults if undetected, contribute to the degradation and eventual failure of the motors. As it is not economical to introduce redundant backup motors, condition monitoring for induction motor is important for safe operation. In order to keep the motor in good condition, techniques such as fault monitoring, detection, classification and diagnosis have become increasingly essential. Earlier detection of the fault reduces repair cost and motor outage time thereby improving safety.

1.1 INDUCTION MOTOR FAULT STATISTICS

The faults that occur in the induction motor can be classified as internal faults and external faults as pointed out by Sinan altug (1999). Different internal motor faults are short circuit of motor leads, inter-turn short – circuits, ground faults, worn-out/broken bearings and broken rotor bars. External motor faults are phase failure, asymmetry of mains supply, mechanical overload, blocked rotor and under-load. Furthermore, the wide variety of environments and conditions that the motors are exposed to can age the motor and make it subject to faults.

Figure 1.1 shows the fault statistics of induction motor given by Ming Xu (1998). The statistical data of failures among utility size motors indicated that 10% of the induction motor failures were rotor related. Rotor related faults in three phase induction motors are due to broken bars and end rings. The root of the failure is the crack that develops in the rotor bars. The crack may increase its size if left undetected.

Broken bars can be a serious problem when Induction motors have to perform hard duty cycles. Broken rotors do not initially cause an Induction motor to fail, but

they can impair motor performance, lead to motor malfunction, and cause severe mechanical damage to the stator winding if left undetected.

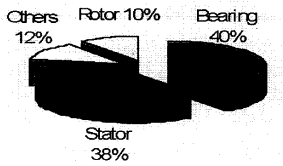

Figure 1.1 Induction Motor Fault Statistics

These faults occur primarily due to the thermal, magnetic, mechanical, environmental stresses that the rotor has to undergo during the routine usage. Faults involving several broken bars cause excessive vibration, noise and sparking during motor starting. The condition can be visualized as continuous increase in rotor bar resistance which increases from its nominal value to infinity when the bar is fully broken. Moreover, an Induction motor with broken bars cannot operate in dangerous environments due to sparking at the fault site. For these reasons, broken rotors should be taken care of during the initial stage itself and further damage can be prevented.

1.2 LITERATURE SURVEY

The manufactures and users of electrical machines initially relied on simple protections such as over-current, over-voltage, earth-fault, etc to ensure safe and reliable operation. However, as the tasks performed by these machines grew increasingly complex; improvements were also sought in the field of fault diagnosis. It has now become very important to diagnose faults at their very inception; as unscheduled machine downtime can upset deadlines and cause heavy financial losses.

As pointed out by Peter Vas (1993), the major faults of electrical machines can broadly be classified as the following:

- Stator faults resulting in the operating or shorting of one or more of a stator phase winding,

- Abnormal connection of the stator windings,
- Broken rotor bar or cracked rotor end-rings,
- Static and/or dynamic air gap irregularities,
- Bent shaft can result in a rub between the rotor and stator, causing serious damage to stator core and windings,
- Shorted rotor field winding, and
- Bearing and gearbox failures.

These faults produce one or more of the symptoms as given below:

- Unbalanced air-gap voltages and line- currents,
- Increased torque pulsations,
- Decreased average torque,
- Increased losses and reduction in efficiency, and
- Excessive heating

Fabricated type rotors have more incidents of rotor bar and end ring breakage than cast rotors. On the other hand, cast rotors are more difficult to repair once they fail. The reasons for rotor bar and end ring breakage are several as pointed out by Filippetti et al (1996).They can be caused by

- Thermal stresses due to thermal overload and unbalance, hot spots or excessive losses, sparking (mainly fabricated rotors),
- Magnetic stresses caused by electromagnetic forces, unbalanced magnetic pull, electromagnetic noise and vibration.
- Residual stresses due to manufacturing problems.
- Dynamic stresses arising from shaft torques, centrifugal forces and cyclic stresses.
- Environmental stresses caused by for example contamination and abrasion of rotor material due to chemicals or moisture,
- Mechanical stresses due to loose laminations, fatigued parts, bearing failure etc.

Different techniques for the detection of broken bars can be summarized as follows:

- Time and frequency domain analysis of induced voltages in search coils placed internally around stator tooth tip and yoke.
- Time and frequency domain analysis of shaft flux or more generally axial leakage flux which is monitored by using an external search coil wound around the shaft of a machine.
- Harmonic analysis of motor torque and speed.
- Vibrational analysis
- Stator current spectrum analysis

In general, condition- monitoring schemes have concentrated on sensing specific failures modes in one of the three induction motor components: the stator, the rotor, or the bearings. Even though the thermal and vibrational monitoring has been utilized for decades, most of the recent research has been directed toward electrical monitoring of the motor with emphasis on inspecting the stator current of the motor. The stator current spectral analysis has the advantage of not requiring any extra sensors in addition. As pointed out by Mohammed EI Hachemi Benbouzid (2003), fault detection based on motor current relies on interpretation of the frequency components in the current spectrum that are related to rotor asymmetries. However, the current spectrum is influenced by many factors, including electric supply, static, and dynamic load conditions, noise, motor geometry and fault conditions. These conditions may lead to errors in fault condition.

With advances in digital technology, adequate data processing capability is now available on cost-effective hardware platforms, to monitor motors for a variety of abnormalities on a real time basis in addition to the normal motor protection function.

1.3 OBJECTIVES

The objectives of the project report are as follows:

- To detect the rotor bar fault in three phase Induction Motor using neural network and fuzzy logic
- To Optimize the fuzzy membership function using genetic algorithm
- Online implementation of the fuzzy logic based fault detection scheme

1.4 ORGANIZATION OF THE PROJECT REPORT

In chapter 1, the problems that occur in the induction machine, the percentage occurrence of various failures, the different techniques used to detect the rotor fault, objectives of the project are discussed. In chapter 2, the operating principle, causes, field distribution, effects of rotor asymmetry in induction motor and the methodology are discussed. In chapter 3, the hardware set up for online monitoring and offline monitoring and the results obtained using FFT analyzer are discussed. In chapter 4, the basics of neural network, back propagation network and the neural network based fault diagnosis are discussed. In chapter 5, the mamdani fuzzy inference system and fuzzy logic based fault diagnosis are discussed. In Chapter 6, the tuning of membership function in fuzzy logic using genetic algorithm for fault detection is discussed.

CHAPTER 2
DETECTION OF ROTOR ASYMMETRY IN CAGE INDUCTION MOTORS

2.1 INTRODUCTION

Three-phase induction machines are asynchronous speed machines, operating below synchronous speed when motoring and above synchronous speed when generating. They are comparatively less expensive to equivalent size from a few watts to some multi mega watts. They indeed, are the workhorses of today's industries. AC motors are rugged and require very little maintenance.

The cage type induction motor has electrical circuits on both sides i.e., on stator and rotor but it is singly fed machine in the sense that all external electrical input into the stator circuit only. There is no external electrical input into the rotor circuit. According to electromagnetic induction principle, the rotor currents are induced by the rotating magnetic field of the stator. This is a great advantage of the machine, that there are no brushes and commutator needed to make electrical connections from stationary environment to the rotating member.

2.2 OPERATING PRINCIPLE

When the stator is energized from a three-phase supply, a rotating magnetic field is created in the air gap of the motor. The rotating magnetic flux will induce voltages in both the stator coils and the rotor coils. The electromagnetic forces resulting from the interaction of the current in the rotor conductors and the air gap flux will result in a torque, which will cause the rotor to rotate.

The basic cause of the creation of the induced voltage, the current and the torque is the relative motion between the air-gap flux and the rotor conductors. Therefore the direction of the rotation will be such that to minimize this relative velocity. In other words, the rotor will rotate in the same direction as the rotating magnetic field. But the rotor speed increases, the relative speed between the rotor conductors and field becomes less and less. Therefore the induced electro motive force (e.m.f.), the current and the resulting torque also become less. There will be no induced e.m.f., if the rotor spins at the synchronous speed, because there will be no

relative motion between the field and the rotor conductors. Typical rotor of an IM is shown in Figure 2.1.

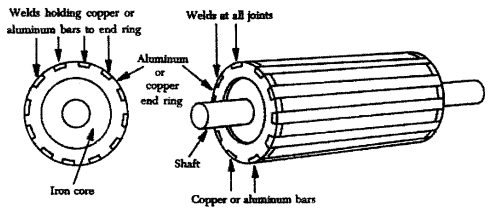

Figure 2.1 Rotor of Induction Motor

Cage rotor design and manufacturing have undergone little change. As a result, rotor failures now account for a large percentage of total induction motor failures. Cage rotors are basically of two types: cast and fabricated. Previously, cast rotors were only used in small machines. However, with the advent of cast ducted rotors; casting technology can be used even for the rotors of machines in tie range of 3000 kW. Fabricated rotors are generally found in larger or special application machines. Cast rotors though more rugged than the fabricated type, can almost never be repaired once faults like cracked or broken rotor bars develop in them.

2.3 CAUSES OF ROTOR ASYMMETRY AND FIELD DISTRIBUTION

As pointed by Peter Vas (1993), in the case of die-cast rotors, asymmetries are due to technological difficulties, or to melting of bars and end-rings. However, failures can also result in rotors not employing die-casting. There are several main reasons for this. Firstly, the bar is smaller than the slot which it fits and this allows radial movement of the bar, particularly during starting, and can lead to fatigue and eventually to the fracture of a bar. Secondly, a rotor bar may be unable to move longitudinally in the slot it occupies, when thermal stresses are imposed upon it, during starting of the machine. Thirdly, during the brazing process in manufacture, non-uniform metallurgical stresses may be built into the cage assembly, and these can

also lead to failure during operation. Finally, heavy end-rings can result in large centrifugal forces, which can cause dangerous stressing of the bars. The copper rotor bars and end-rings of squirrel-cage motors may also break as a consequence of all types of heavy operation conditions (e.g. cycle stresses), or due to the misuse of the motor (e.g. excessive number of consecutive direct-on-line starting, where the large starting currents product large mechanical and thermal stresses on the cage).

Rotor cage asymmetry results in the asymmetrical distribution of the rotor currents, and due to this, damage of one rotor bar can cause the damage of surrounding bars, and thus the damage can spread, leading to multiple bar fractures. In case of a crack, which occurs in a bar (e.g. at an end-ring-to-bar joint), the cracked bar will overheat, and this can cause the bar to break. Thus the surrounding bars will carry higher currents and therefore they are subjected to even larger thermal and mechanical stresses, and they can start to crack etc. Most of the current which would have flowed in the broken bar will flow in the two bars adjacent to it. The large thermal stresses may also damage the rotor laminations. The temperature distribution across the rotor lamination is also changed due to the rotor asymmetry (this could be monitored by using invasive techniques, e.g. by using thermocouples embedded around the rotor stack).

The cracking of the bars can be present at various locations, including the slot portion of the bars under consideration and the end-ring-to-bar joints. The possibility of cracking in the region of the end-ring-to-bar joints is the greatest when the start-up time of the machine is long, and when frequent starts are required.

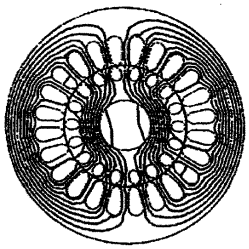

Figure 2.2 Magnetic Field Distributions in Healthy Motor

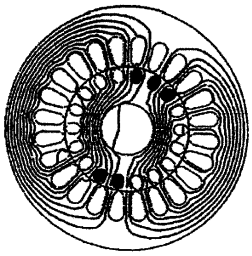

Figure 2.3 Magnetic Field Distributions with 5 Bars Broken

The Figure 2.2 shows the magnetic field distribution around the rotor of induction motor with no broken bars. The field is continuous without any distortion. The Figure 2.3 shows the field distribution under faulty condition. This varies the magneto motive force (m.m.f) distribution and causes harmonics in the stator current as given by Mohammed EI Hachemi Benbouzid (2000).

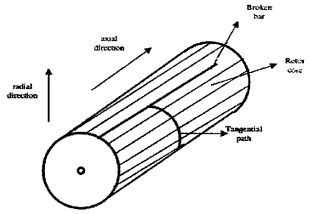

Figure 2.4 Typical Rotor of IM with One Broken Bar.

Figure 2.4 shows a typical skewed rotor of an induction motor with one broken rotor bar in cylindrical coordinates. Since the stator windings, the rotor bars, and the rotor core between the uninsulated rotor bars is considered to be the current flow paths, the machine can be divided axially into sections as pointed by Homayoun Meshgin – Kelk et al (2004). The field within each section is assumed to be axially uniform.

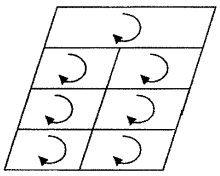

Figure 2.5 Electrical Equivalent of the Rotor with One Broken Bar

Figure 2.5 shows the electrical equivalent circuit of a portion of the rotor just near the bar breakage and its assigned mesh currents. The rotor has been divided into four layers in the axial direction.

The m.m.f produced by the stator currents and the rotor mesh currents act on the radial axis. This m.m.fs produces fluxes that have three components in the cylindrical coordinates. The first component is the radial component that flows through the stator teeth, the air gap, and the rotor teeth. The second component is the axial component that flows through the stator frame, the rotor shaft, and the axial leakage paths. Finally, the circumferential component flow through the stator and the rotor yokes, the stator and the rotor slot openings, and the other leakage paths. Because of the laminated core used in the stator and in the rotor, the magnetic fluxes produced by the inter-bar currents can only pass through the stator frame and the rotor shaft.

2.4 EFFECTS OF ROTOR ASYMMETRY

A three-phase induction machine is assumed in the steady-state. It is assumed that the m.m.f distribution is sinusoidal and the only asymmetry is present on the rotor, and the stator is supplied by a symmetrical three-phase voltage system. Due to the asymmetry in the rotor circuit, the rotor currents will produce positive and negative-sequence rotor m.m.f.s. Since the angular frequency of the rotor currents is sf, where f is the supply frequency and s is the slip, the angular speed of the positive-sequence rotor m.m.f with respect to the stator is

$$f_r + sf = f(1-s) + sf = f \qquad (2.1)$$

and the angular speed of the negative-sequence rotor m.m.f. with respect to the stator is $f_r - sf = f(1-s) - sf = (1-2s)f$ (2.2)

It follows that the positive-sequence rotor currents I_{r1} result in positive-sequence e.m.f.s and currents in the stator winding of angular frequency f and the negative-sequence rotor currents I_{r2} result in negative-sequence e.m.f.s and negative-sequence currents in the stator windings of angular frequency (1 – 2s)f. Since the angular frequencies of the positive- and negative-sequence stator currents ($\bar{I}_{s1}$, $\bar{I}_{s2}$) differ by 2sf oscillations are present in the stator currents.

The steady-state electromagnetic torque T_e of the machine is equal to the sum of the positive- and negative-sequence torque components T_{e1} and T_{e2}, and the torque components can be immediately obtained by considering the positive – and negative-sequence air-gap powers. The positive-sequence air-gap power P_{g1} is equal to the positive-sequence input power minus the positive-sequence stator rotor losses, and the negative-sequence air-gap power P_{g2} is equal to the negative value of the negative-sequence stator losses across the resistance $R_s / (1-2s)$. Thus the net average torque in the steady-state can be expressed as

$$T_e = T_{e1} + T_{e2} \qquad (2.3)$$

Where

$$T_{e1} = P_{g1} / f = (3/f)\, \mathrm{Re}\,[(\bar{U}_{s1}^{*}\, \bar{I}_{s1}) - 3|\bar{I}_{s1}|^2 R_s] \qquad (2.4)$$

$$T_{e2} = P_{g2} / f = -(3/f)\, |\bar{I}_{s2}|^2 R_s / (1-2s) \qquad (2.5)$$

In equations (2.4), (2.5), $\bar{U}_{s1}$ is the positive-sequence stator voltage, and $|\bar{I}_{s1}|$ and $|\bar{I}_{s2}|$ are the moduli of the positive- and negative-sequence stator currents respectively. The positive- and negative-sequence rotor ohmic losses are obtained as

$$P_{r1} = s\, P_{g1} \qquad (2.6)$$

$$P_{r2} = (1-2s)\, P_{g2} \qquad (2.7)$$

The stator positive- and negative-sequence ohmic losses are

$$P_{s1} = 3|\bar{I}_{s1}|^2 R_s \qquad (2.8)$$

$$P_{s2} = 3|\bar{I}_{s2}|^2 (R_s + R_N)/(1-2s) \qquad (2.9)$$

where R_N is the resistance of the network connected to the stator terminals of the machine.

Due to rotor asymmetry, pulsating torques are produced in the developed electromagnetic torque. In the steady-state, the frequency of the torque pulsations is 2sf. This is due to the fact that the difference between the angular frequencies of the positive- and negative-sequence stator currents is

$$f - (1-2s)\, f = 2sf \qquad (2.10)$$

The pulsating torques is superimposed on the average main torque .The mean value of the pulsating torque component is zero: it does not contribute to the motor output, but is causes undesirable noise and vibration. This pulsating torques is even undesirable when their amplitudes are small, as resonance occurs, when the frequency of the pulsations is equal to the natural frequency of the induction motor. If the induction motor is controlled in a wider speed range, or during starting, pulsating torques are of greater importance, as they also pass the natural frequencies. In contrast to the average torque, whose amplitude is the largest around the half-speed region, at half synchronous speed, the amplitudes of the pulsating torque is small.

2.5 METHODOLOGY

The Figure 2.6 shows the rotor fault detection process carried in this project. The voltage from the induction motor is measured and the Fast Fourier Transformation (FFT) analysis is done. The output of FFT is used for fault diagnosis using neural network and fuzzy logic.

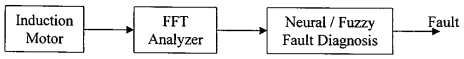

Figure 2.6 Rotor Fault Detection Process

The fault detection process is carried out in two ways

1) Offline monitoring
2) Online monitoring

2.5.1 Offline Monitoring

The motor is disconnected from the supply, and the induced voltage in the stator due to rotor flux is utilized to detect the fault. If there is any broken bar, it will directly affect the induced voltages in the stator windings. The stator current spectrum is converted in to an equivalent voltage and recorded by giving it as the input to the microphone input terminal of the PC by means of a stereo cable. Using the FFT analyzer the spectral values is obtained and the required side band at (1± 2s)f value is measured.

2.5.2 Online Monitoring

In running condition, the fault is detected. The stator current spectrum is converted in to an equivalent voltage and recorded by giving it as the input to the microphone input terminal of the PC by means of a stereo cable. Using the FFT analyzer the spectral values is obtained and the required side band at (1± 2s)f value is measured.

CHAPTER 3
EXPERIMENTAL SETUP FOR DATA ACQUISITION

3.1 INTRODUCTION

In case of an Induction motor, the 3-phase symmetrical stator winding fed from a symmetrical supply with frequency f, will produce a resultant forward rotating magnetic field at synchronous speed and if exact symmetry, exists there will be no resultant backward rotating field. Any asymmetry of the supply or stator winding impedances will cause a resultant backward rotating field from the stator winding. When applying the same rotating magnetic field fundamentals to the rotor winding, the first difference with respect to the stator, induced e.m.f and current in the rotor winding is at slip frequency i.e. sf, and not at the supply frequency.

The rotor currents in a cage winding produce an effective 3-phase magnetic field with the same number of poles as the stator field but rotating at slip frequency f_r = sf with respect to the rotating rotor. With a symmetrical cage winding, only a forward rotating field exists. If rotor asymmetry occurs then there will also be a resultant backward rotating field at slip frequency with respect to the forward rotating rotor. As a result, the backward rotating field with respect to the rotor induces an e.m.f. and current in the stator winding at frequency f_1.

$$f_1 = f(1-2s)\ \text{Hz} \qquad (3.1)$$

This is referred to as the lower slip frequency sideband due to broken rotor bars. Therefore, there is a cyclic variation of current that causes a torque pulsation at twice slip frequency (2sf) and a corresponding speed oscillation, which is also a function of the drive inertia.

This speed oscillation can reduce the magnitude of the (1-2s)f sidebands but an upper sideband current component at (1+2s)f is induced in the stator winding due to rotor oscillation. The upper sideband is enhanced by the third time harmonic flux.

Broken rotor bars therefore result in current components being induced in the stator winding at frequencies given by:

$$f_{1,2} = f(1\pm 2s)\ \text{Hz} \qquad (3.2)$$

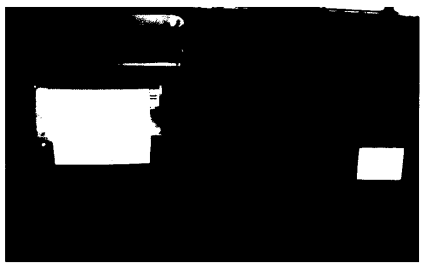

Figure 3.1 Experimental Setup for Rotor Fault Detection

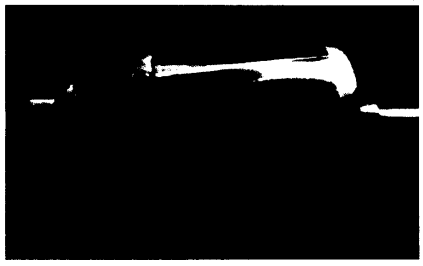

Figure 3.2 Broken Bar

These are the slip frequency sidebands due to broken rotor bars. These two frequency components show predominant variation in their amplitudes and these two components are taken for the analysis under various broken bar conditions.

3.2 EXPERIMENTAL SETUP FOR OFFLINE MONITORING

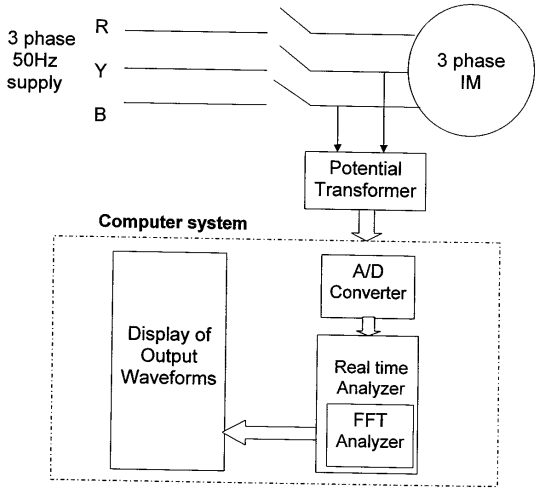

Figure 3.3 Experimental Setup for Offline Monitoring

The broken rotor bars can be detected by analyzing the voltage induced in the stator windings when the supply is disconnected. The Figure 3.3 shows the experimental setup for offline monitoring. When the source of an operating induction machine is detached, the stator currents rapidly die down to zero. Then, the only source to induce voltage in stator windings is the rotor currents. If there are some broken rotor bars, they will directly affect the induced voltages in the stator windings.

In the case of a healthy machine with no broken bars, m.m.f produced by the rotor bar current at disconnection of the stator phases is predominantly sinusoidal. Thus, the voltage induced in the stator due to this m.m.f should not have significant

harmonic content other than the fundamental and that due to the stepped rotor current distribution. However, with one or more rotor bars broken, the rotor m.m.f wave shape will deviate from its sinusoidal nature under healthy conditions, and these distortions can be picked up in the induced stator voltage, even under no-load conditions.

3.3 EXPERIMENTAL SETUP FOR ONLINE MONITORING

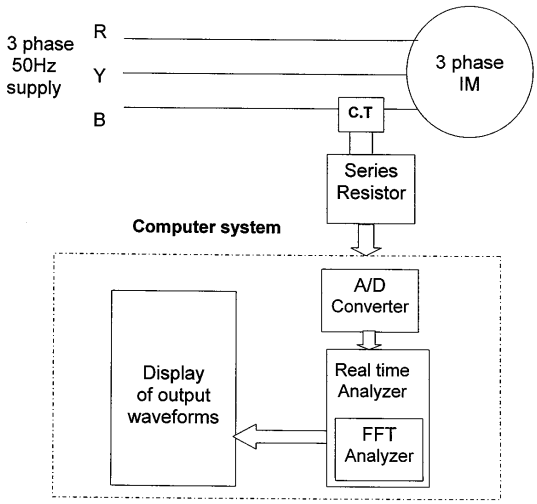

Figure 3.4 Experimental Setup for Online Monitoring

In online monitoring the fault is analyzed in the running condition. The stator line current is being monitored by converting it into an equivalent voltage by means of a current transformer and a series resistor. Then the waveform is analyzed using

FFT to measure the amplitude of the side band harmonics. The block diagram is shown in Figure 3.4.

3.4 COMPONENT DESCRIPTION

3.4.1 Induction Motor

The motor used for this purpose is a 3-phase squirrel cage Induction motor. The rotor being casted type made of Aluminum moulded bars. Totally there are 28 rotor bars and the analysis is done up to 3 broken bars. The normal voltage across any two stator terminals after supply disconnection being 7V rms and it reduces as the speed of the rotor also reduces.

Motor Specifications

Power	:	1HP
Rated Voltage	:	415 V
Rated Speed	:	960 rpm
Poles	:	6
No load current	:	1.2 A
No of rotor bars	:	28

3.4.2 Potential Divider

In order to analyze the stator current pattern, the stator current is converted to an equivalent voltage by means of a potential divider. The circulating current in the stator windings is 20mA. The converted voltage is given as the input to the microphone terminal of the PC. In order to make the input voltage to compatible level of PC's sound card it is reduced to about 1V (peak to peak) by adjusting the potential divider.

3.4.3 Stereo Cable

The input voltage is given to the PC's microphone input terminal by means of a stereo cable. Since the voltage is already stepped down to compatible level, there is no need of any ohmic connector to limit the voltage.

3.4.4 Current Transformer

The current transformer of transformation ratio 100:5 is used. The no load line current of 1.2A is stepped down to 50mA and it is converted into an equivalent voltage 1 by connecting a resistor in series with the secondary coil. This is used only for the on line monitoring of fault.

3.4.5 A/D Converter

By means of the stereo cable the analog voltage is given to the sound card. It is converted to a digital form by means of an inbuilt 16 bit A/D converter.

3.4.6 Real Time Analyzer

The stator current spectrum is converted into an equivalent voltage and recorded in the PC by means of a stereo cable through the microphone input terminal. The input voltage level to the PC sound card is adjusted by means of a potential divider to the acceptable level of the sound card. It is normally 1V (peak to peak). The waveforms are recorded for various numbers of broken bars. In order to perform FFT analysis on the input waveform a software "real time analyzer" is used. It permits the analog waveform to be directly recorded by the PC. It is a part of "Acoustic Analyzing System" which mainly analyzes sound waveforms. The main advantage of using this software is that it permits the analog waveform to be recorded directly and it is digitized by means of inbuilt A/D converter of the PC's sound card.

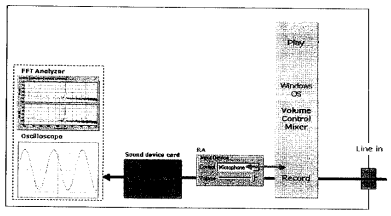

Figure 3.5 Block diagram of the sound card in PC

The Figure 3.5 shows the block diagram of the sound card of the PC along with the control by real time analyzer. The voltage input to the microphone input terminal is being recorded by the windows operating system, volume control mixer. The input voltage level can be varied by means of volume control. Then the analog voltage signal is digitized by means of an inbuilt A/D converter. Then the voltage waveform is displayed in the oscilloscope window as like in the ordinary digital storage oscilloscope. The time range of the input signal can be varied in the oscilloscope. Further analysis can be performed by making use of the stored wave in wave file format. The output of the FFT analyzer will be in one of the following forms: spectrum, octave band or waterfall model. It will be an amplitude Vs frequency graph. The amplitude of the various frequency components are displayed in dB. The values can also be recorded by means of using the option data recorder provided by the FFT analyzer. The amplitudes of the two side band components at frequencies (1+2s)f and (1-2s)f for various broken bar conditions are measured.

The diagnosis of the faults is done using neural network and fuzzy logic. Fuzzy logic based system is successfully implemented to classify broken rotor bar faults by categorizing the (1±2s)f components by a set of rules.

3.5 EXPERIMENTAL RESULTS

3.5.1 Offline Monitoring

The stator voltage across the stator terminals are analyzed for various number of broken rotor bars after supply disconnection. The voltage across the stator terminal of healthy machine and the machine with broken bar are shown in Figures (Figure3.6 to Figure3.9).

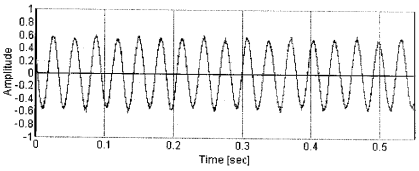

(a) Sinusoidal Voltage of the Healthy Machine

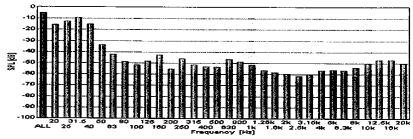

(b) The Voltage across the Stator Terminal with FFT Analyzer

Figure 3.6 The Voltage across the Stator Terminal of Healthy Machine

By comparing the stator sinusoidal voltage the difference cannot be noticed. So FFT analysis is done in all the cases to identify the variations in the harmonic amplitude.

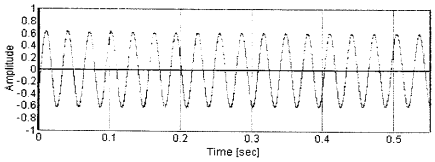

(a) Sinusoidal Voltage with One Broken Bar

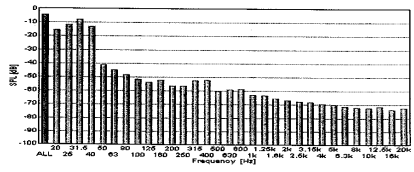

(b) The Voltage across the Stator Terminal with FFT Analyzer

Figure 3.7 The Voltage across the Stator Terminal with One Broken Bar

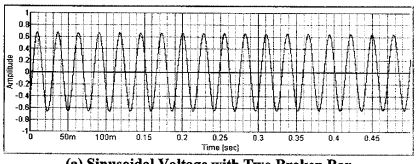

(a) Sinusoidal Voltage with Two Broken Bar

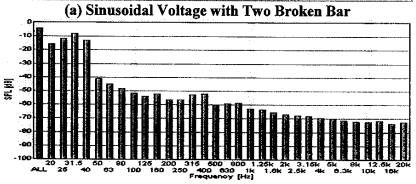

(b) The Voltage across the Stator Terminal with FFT Analyzer

Figure 3.8 The Voltage across the Stator Terminal withTwo Broken Bar

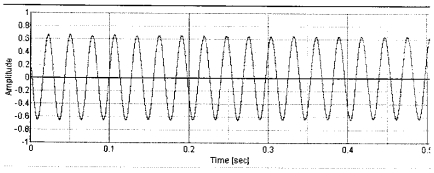

(a) Sinusoidal Voltage with Three Broken Bar

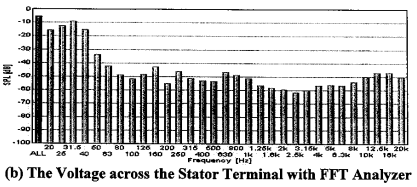

(b) The Voltage across the Stator Terminal with FFT Analyzer

Figure 3.9 The Voltage across the Stator Terminal with Three Broken Bar

The output of the FFT analyzer will be an amplitude Vs frequency graph in octave band as shown in the Figures (Figure 3.6(b) – Figure 3.9(b)). For analysis, the two side band components of frequency (1-2s)f and (1+2s)f are considered and the values are denoted as amplitudes A_1 and A_2 respectively and tabulated in Tables (Table 3.1 – Table 3.4). The amplitudes of the side bands are noted in dB at a specific speed of the rotor under various broken bar conditions. So the frequency of the stator current will be the same in all the cases.

Table 3.1 Harmonic Amplitudes of Healthy Machine

Time in sec	Speed rpm	A_1 dB	A_2 dB
1	893	-18.82	-22.93
2	820	-14.43	-28.35
3	**750**	**-12.59**	**-29.55**
4	677	-10.34	-36.26
5	610	-9.83	-38.44
6	546	-10.02	-42.74
7	487	-10.85	-44.46
8	430	-12.28	-44.05
9	377	-14.23	-43.89
10	327	-16.77	-44.13

Table 3.2 Harmonic Amplitudes of Machine with One Broken Bar

Time in sec	Speed rpm	A_1 dB	A_2 dB
1	890	-21.26	-19.75
2	816	-15.88	-24.59
3	**749**	**-12.12**	**-32.49**
4	680	-10.51	-34.6
5	615	-9.37	-36.55
6	540	-8.91	-40.83
7	480	-9.06	-48.38
8	428	-9.72	-61.01
9	376	-10.8	-57.98
10	337	-12.33	-56.54

Table 3.3 Harmonic Amplitudes of Machine with Two Broken Bar

Time in sec	Speed rpm	A_1 dB	A_2 dB
1	900	-22.29	-18.75
2	824	-16.83	-23.59
3	**751**	**-12.78**	**-31.65**
4	678	-11.53	-33.6
5	608	-10.34	-35.53
6	540	-9.96	-39.86
7	476	-10.03	-47.31
8	415	-10.78	-60.14
9	358	-11.12	-56.45
10	305	-13.45	-55.67

Table 3.4 Harmonic Amplitudes of Machine with Three Broken Bar

Time in sec	Speed rpm	A_1 dB	A_2 dB
1	908	-21.45	-19.12
2	845	-15.23	-24.76
3	**750**	**-12.35**	**-30.91**
4	655	-10.48	-34.15
5	595	-9.92	-36.17
6	535	-8.15	-40.25
7	478	-9.38	-48.17
8	423	-9.19	-61.28
9	371	-10.12	-57.38
10	322	-12.14	-56.25

Table 3.5 Harmonic Amplitudes for Various Broken Bar in Offline Method

Number of broken bars	A_1 in dB	A_2 in dB
0	-12.59	-29.55
1	-12.12	-32.49
2	-12.78	-31.65
3	-12.35	-30.91

The selected speed is 750 rpm and the frequency at that instant is 32 Hz. The frequencies of the side bands as per the Equation (3.2) will be 16Hz and 48Hz and the corresponding amplitude is shown in Table 3.5. A_1 and A_2 are the amplitudes of the side band harmonics which are taken for further diagnosis.

3.5.2 Online Monitoring

In this case any instant of stator current can be used, as the amplitude and frequency of the stator current is always the same. The voltage across the stator terminal of healthy machine and the machine with broken bar are shown in Figures (Figure 3.10 - Figure 3.13).

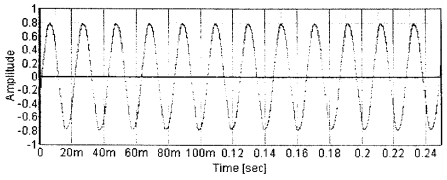

(a) Sinusoidal Voltage of the Healthy Machine

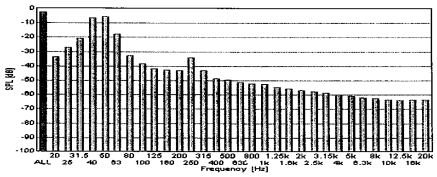

(b) The Voltage across the Stator Terminal with FFT Analyzer

Figure 3.10 The Voltage across the Stator Terminal of Healthy Machine

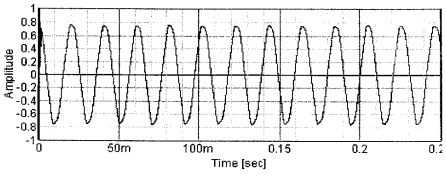

(a) Sinusoidal Voltage with One Broken Bar

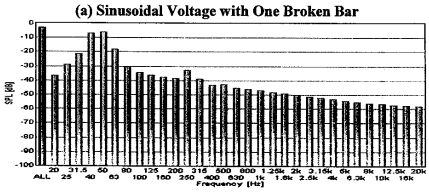

(b) The Voltage across the Stator Terminal with FFT Analyzer

Figure 3.11 The Voltage across the Stator Terminal with One Broken Bar

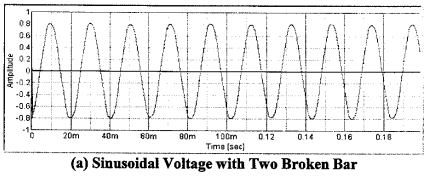

(a) Sinusoidal Voltage with Two Broken Bar

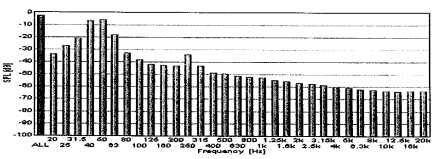

(b) The Voltage across the Stator Terminal with FFT Analyzer

Figure 3.12 The Voltage across the Stator Terminal with Two Broken Bar

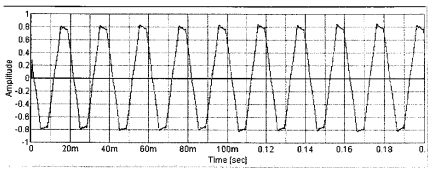

(a) Sinusoidal Voltage with Three Broken Bar

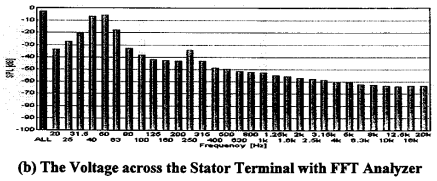

(b) The Voltage across the Stator Terminal with FFT Analyzer

Figure 3.13 The Voltage across the Stator Terminal with Three Broken Bar

Table 3.6 Harmonic Amplitudes for Various Broken Bar in Online Method.

Number of broken bars	A_1 in dB	A_2 in dB
0	-11.13	-10.55
1	-11.35	-10.77
2	-11.06	-10.46
3	-10.93	-9.74

For analysis, the two side band components of frequency (1-2s)f and (1+2s)f are considered and the values are denoted as amplitudes A_1 and A_2 respectively and tabulated in Table 3.6. A_1 and A_2 are used for fault diagnosis using neural network and fuzzy logic.

CHAPTER 4

NEURAL NETWORK BASED FAULT DIAGNOSIS

4.1 INTRODUCTION TO NEURAL NETWORK

An artificial neural network is an information processing system that has certain performance characteristics in common with biological neural networks. Laurene Fausett (2004) explains that the artificial neural networks have been developed as generalization of mathematical models of human cognition or neural biology, based on assumptions that:

- Information processing occurs at many simple elements called neurons.
- Signals are passed between neurons over connection links.
- Each connection link has as associated weight, which, in a typical neural net, multiplies the signal transmitted.
- Each neuron applies an activation function (usually nonlinear) to its net input (sum of weighted input signals) to determine it output signal.

A biological neuron has three types of components that are of particular interest in understanding an artificial neuron: its dendrites, soma and axon. Dendrites receive signal from other neurons. The signals are electrical impulses that are transmitted across a synaptic gap by means of a chemical process. The soma or cell body sums the incoming signals. When sufficient input is received, the cell fires; that is, it transmits a signal over its axon to other cells. Figure 4.1 shows the structure of biological neuron.

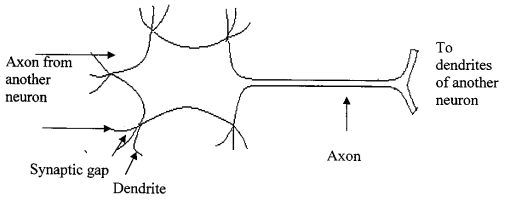

Figure 4.1 Structure of Biological Neuron

An Artificial Neural Network is characterized by,

- Its pattern of connections between the neurons (called its architecture)
- Its method of determining the weights on the connections (called its training or learning, algorithm), and
- Its activation function

The network function is determined largely by the connections between elements. Therefore, a neural network can be trained to perform a particular function by adjusting the values of the connections (weight) between the elements commonly neural networks are adjusted, or trained, so that a particular input leads to a specific target output. Figure 4.2 shows the basic operation of a neural network.

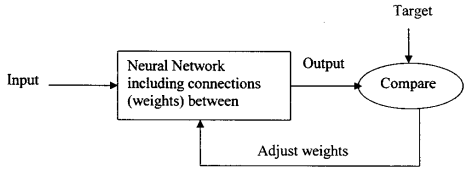

Figure 4.2 Basic Operation of Neural Network

There, the network weight is adjusted based on a comparison of the output and the target, until the network output matches the target.

4.1.1 Neuron Model

Figure 4.3 shows a neuron with a single scalar input with no bias. The scalar input p, is transmitted through a connection that multiplies its strength by the scalar weight w, to form the product wp, again a scalar. Here the weighted input wp is the only argument of the activation function f, which produces the scalar output a.

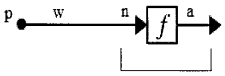

Neuron without bias

a = f (wp)

Figure 4.3 Single – Input Neuron without Bias

Figure 4.4 shows a neuron with a scalar input, with scalar bias. The bias is much like a weight, except that it has a constant input of 1. The activation function

net input n, again a scalar, is a sum of the weighted input wp and the bias b., this sum is the argument of the activation function f. f is an activation function, typically a step function or a sigmoid function, that takes the argument n and produces the output a. w and b are both adjustable parameters of the neuron.

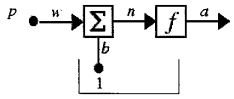

Neuron with bias

a = f (wp + b)

Figure 4.4 Single Input Neuron with Bias

The central idea of neural networks is that such parameters can be adjusted so that the network exhibits some desired or interesting behavior. Thus, we can train the network to do a particular job by adjusting the weight or bias parameters, or perhaps the network itself will adjust these parameters to achieve some desired end.

4.1.2 Activation Functions

An activation function may be linear or a non-linear function of an. A particular activation function is chosen to satisfy some specification of a problem that the neuron is attempting to solve. There are three most commonly used activation function. They are

(a) Hard limit activation function
(b) Linear activation function
(c) Log-sigmoid activation function

(a) Hard limit activation function:

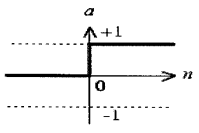

a = hardlim (n)

Figure 4.5 Hard Limit Activation Function

Figure 4.5 shows the graphical representation of the hard limit activation function. The hard limit activation function sets the output of the neuron to 0 if the function argument is less than 0, or 1 if its argument is greater than or equal to 0.

(b) Linear activation function:

The output of a linear activation function is equal to its input. The output (a) versus input (p) characteristic of a single-input linear neuron is shown in Figure 4.6.

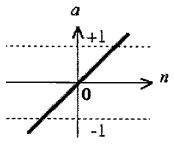

a = purelin (n)

Figure 4.6 Linear Activation Function

(c) Log-sigmoid activation function:

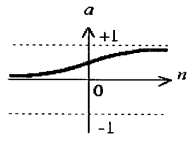

a = logsig (n)

Figure 4.7 Log-Sigmoid Activation Function

Figure 4.7 shows the log-sigmoid activation function. This activation function takes the input (which may have any value between plus and minus infinity) and squashes the output into the range 0 to 1, according to expression

$$a = 1 / 1 + e^{+n} \qquad (4.1)$$

This activation function is commonly used in multilayer networks that are trained using the back-propagation algorithm, in part because this function is differentiable.

4.1.3 Learning Rules

The weights and biases of the network can be modified by means of 'learning rule'. This procedure may also be referred to as a training algorithm. The purpose of the learning rule is to train the network to perform some task. Neural networks can be trained to solve problem that are difficult for conventional computers or human beings. There are many types of neural network learning rules. They fall into three broad categories: supervised learning, unsupervised learning and reinforcement (or graded) learning.

(a) Supervised learning: In supervised learning, the network is provided with inputs and the corresponding correct output. As the inputs are applied to the network, the network outputs are compared to the targets. The learning rule is then used to adjust the weights and biases of the network in order to move the network outputs closer to the targets. An example for the supervised learning is the perceptron-learning rule.

(b) Reinforcement learning: This is similar to supervised learning, except that, instead of being provided with the correct output for each network input, the algorithm is only given a grade. The grade is a measure of the network performance over some sequence of inputs. This type of learning is currently much less common than supervised learning.

(c) Unsupervised learning: In unsupervised learning, the weights and biases are modified in response to network inputs only. There are no target outputs available. The network learns to categorize the input patterns into a finite number of classes. An example for unsupervised learning algorithm is Adaptive Resonance Theory.

4.2 BACK-PROPAGATION NEURAL NETWORK

In supervised learning, the first learning rule is perceptron-learning rule, in which the learning rule is provided with a set of examples of proper network behavior. As each input is applied to the network, the learning rule adjusts the network parameters so that the network output will move closer to the target. The perceptron learning rule is very simple, but it is also quite powerful. This rule will always converge to a correct solution, if such a solution exists. The perceptron-learning rule forms the basis for understanding the more complex networks. As with

the perceptron rule, the Least Mean Square (LMS) algorithm is an example of supervised training. The LMS algorithm will adjust the weights and biases to minimize the mean square error, where the error is the difference between the target output and the network output. The perceptron-net is incapable of implementing certain elementary functions. These limitations were overcome with improved (multilayer) perceptron networks.

Performance learning is another important class of learning law, in which the network parameters are adjusted to optimize the performance of the network. Back propagation (BP) algorithm can be used to train multilayer networks. As with the LMS learning law, BP is an approximate steepest descent algorithm, in which the performance index is mean square error. The difference between the LMS algorithm and back propagation is only in the way in which the derivatives are calculated. The single-layer perceptron like networks are only able to solve linearly separable classification problems. Multilayer perceptron, trained by BP algorithm were developed to overcome these limitations and is currently the most widely used neural network. In addition, multi-layer networks can be used as universal function approximators. A two-layer network, with sigmoid-type activation functions in the hidden layer, can approximate any practical function, with enough neurons in the hidden layer. The Figure 4.8 shows the Architecture of BP Neural Network.

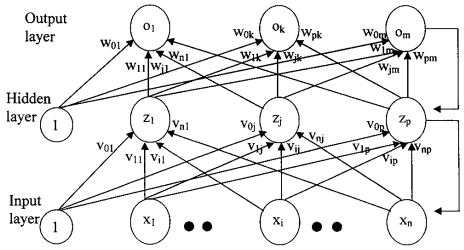

Figure 4.8 Architecture of BP Neural Network

The BP algorithm uses the chain rule in order to compute the derivatives of the squared error with respect to the weights and biases in the hidden layers. It is called BP because the derivatives are computed first at the last layer of the network, and then propagated backward through the network, using the chain rule, to compute the derivatives in the hidden layers.

The BP training algorithm is an interactive gradient algorithm designed to minimize the mean square error between the actual output of a feed-forward net and the desired output. Figure 4.9 shows the flowchart of the BP training algorithm. Let x_i, z_j, o_k be the input, hidden and output layer neuron, v_{oj} and w_{ok} are the bias of input and hidden layer, v_{ij} and w_{jk} are the weights of the input to hidden and hidden to output layer.

Step 1: *Initialize weights and offsets*: set all weights and units offsets to small random values.

Step 2: *Present input and desired output*: Present a continuous valued input vector and specify the desired outputs.

Step 3: *Calculate actual outputs*: For each hidden layer neuron denoted as z_j, j = 1, 2 …p

$z_{ij} = v_{oj} + \sum x_i v_{ij}$; $z_j = f(z_{ij})$

broadcast z_j to the next layer for each output neuron o_{pj}

$o_{jk} = w_{ok} + \sum z_j w_{jk}$; $o_{pj} = f(o_{jk})$

Step 4: *Adapt weights*: Use the recursive algorithm starting at the output units and working back to the first hidden layer. Adjust the weights by

$w_{ji}(t+1) = w_{ji}(t) + \Delta_p w_{ji}(t)$

Where $\Delta_p w_{ji}(t) = \eta \delta_{pj} o_{pi}$, $w_{ij}(t)$ is the weight, η is the learning rate and δ_{pj} is an error term for unit j.

If the unit j is an output unit, then δ_{pj} can be computed by

$\delta_{pj} = (t_{pj} - o_{pi}) f_j(net_{pj})$

If unit j is an internal hidden unit, then δ_{pj} can be computed by

$\delta_{pj} = f_j(net_{pj}) \sum \delta_{pk} w_{kj}$

Step 5: *Training pattern*: The weights are updated using batch training. In batch mode, the weights and biases of the network are updated only after the entire training set has been applied to the network. The gradients calculated at each training example are added together to determine the change in the weights and biases.

Step 6: *Iteration*: As long as the error for the training-testing patterns decreases, training continues. When the error begins to increase, the net is starting to memorize the training patterns too specifically. At this point, training is terminated.

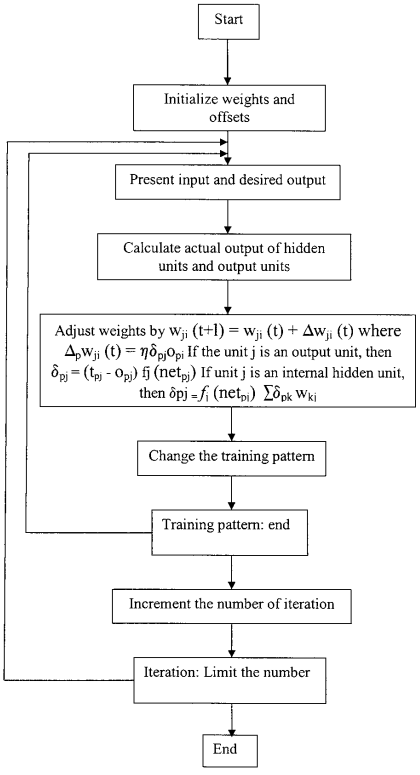

Figure 4.9 Flowchart of BP Training Algorithm

4.3 CHOICE OF PARAMETERS FOR NETWORK TRAINING

When the basic BP algorithm is applied to a practical problem the training may take days or weeks of computer time. This has encouraged considerable research on methods to accelerate the convergence of the algorithm. The research on faster algorithms falls roughly into two categories; the first category involves the development of heuristic techniques, which arises out of a study of the distinctive performance of the standard BP algorithm. These heuristic techniques include such ideas varying the learning rate, using momentum and rescaling variables. Another category of research has focused on standard numerical optimization techniques.

4.3.1 Learning Rate

The speed of training the BP network is improved by changing the learning rate during training. Increasing the learning rate on flat surfaces and then decreasing the learning rate when slope increases can increase the process of convergence. If the learning rate is too large, it leads to unstable learning. And if it is too small, it leads to incredibly long training times. Hence care has to taken while deciding learning rate. There are many different approaches for varying the learning rate. The learning rate is varied according to the performance of the algorithm. The rules of the variable learning rate BP algorithm are:

1. If the squared error increases by more than some set percentage ξ (typically one to five percent) after weight update, then the weight update is discarded, the learning rate is multiplied by some factor $o < p < l$, and the momentum coefficient γ (if it is used) is set to zero.

2. If the squared error decreases after a weight update, then the weight update is accepted and the learning rate is multiplied by some factor $\eta > l$. If γ has been previously set to zero, it is reset to its original value.

3. If the squared error increases by less than ξ then the weight update is accepted but the learning rate is unchanged. If γ has been previously set to zero, it is reset to its original value.

4.3.2 Momentum Factor

In BP with momentum, the weight change is in a direction that is a combination of the current gradient and the previous gradient. This is a modification of gradient descent whose advantage arises chiefly when some training data are very different from the majority of the data. By the use of momentum larger training rate can be used, while maintaining the stability of the algorithm. Another feature of momentum is that it tends to accelerate convergence when the trajectory is moving in a consistent direction. The larger the value of γ, the more the momentum the trajectory has. The momentum coefficient is maintained with the range [0, 1].

4.4 STRUCTURE OF BP NETWORK FOR FAULT DETECTION

An artificial neural network is composed of neurons with a deterministic activation function. The neural network is trained by adjusting the numerical value of the weights will contain the non-linearity of the desired mapping, so that difficulties in the mathematical modeling can be avoided. The BP training algorithm is used to adjust the numerical values of the weights and the internal threshold of each neuron. The network is trained by, initially selecting small random weights and internal threshold and then presenting all training data. Weights and thresholds are adjusted after every training example is presented to the network, until the weight converges or the error is reduced to acceptable value. Figure 4.10 shows the structure of BP Network for Fault Detection.

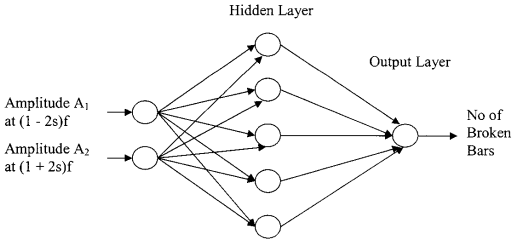

Figure 4.10 Structure of BP Network for Fault Detection

Fault detection neural network consists of two layers: hidden layer and the output layer. There are five neurons in the hidden layer for both offline and online method. The inputs to the neural network are the amplitude A1 at (1-2s)f and A2 at (1+2s)f and the output is the number of broken bars.

4.5 SIMULATION RESULTS

4.5.1 Offline monitoring

4.5.1.1 Training

Feed forward neural networks with two layers are used. The network consists of two input vector, five hidden neurons and one output neuron. BP algorithm is used for training. The activation function in the first layer is log-sigmoid, and the output layer transfer function is tan-sigmoid. The training function used is trainlm. The data from the healthy machine and the data during the fault are given as input to the network. The network is trained with the data given in the Table 3.5. The targets are specified as supervised learning is used.

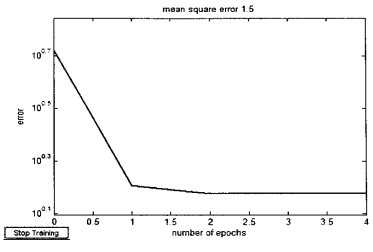

Figure 4.11 Epoch Vs Error Characteristics

Figure 4.11 shows the training error as the function of number of epochs for the network having five hidden layer neuron with the momentum of 0.5 and the number of epochs being 4.

4.5.1.2 Test Results

The test data are given to the network. The difference between the measured and the estimated number of bars is an estimate of fault severity. Once all the datasets are stored in the learning stage, and the network is trained, then by giving the

corresponding inputs to the network, the output of the network gives the value of number of broken bars.

Table 4.1 Test Results

Input A1 (Db)	Input A2 (Db)	Target Output	Actual Value	% error
-12.59	-29.55	0	1.53e-009	1
-12.12	-32.49	1	1	0
-12.78	-31.65	2	1	50
-12.35	-30.91	3	1	66.66
			Average error	29.4

The Table 4.1 gives the test results. Neural network diagnoses require large number of data to train. From the simulation results it is inferred that the percentage error is more.

4.5.2 Online monitoring

4.5.2.1 Training

Feed forward neural networks with two layers are used. The network consists of two input vector, five hidden neurons and one output neuron. BP algorithm is used for training. The activation function in the first layer is log-sigmoid, and the output layer transfer function is tan-sigmoid. The training function used is trainlm. The network is trained with the data given in the Table 3.6.

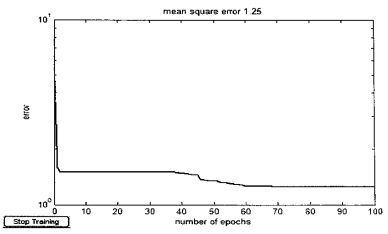

Figure 4.12 Epoch Vs Error Characteristics

Figure 4.12 shows the training error as the function of number of epochs for the network having five hidden layer neuron with the momentum of 0.5 and the number of epochs being 100.

4.5.2.2 Test Results

The test data are given to the network. The difference between the measured and the estimated number of bars is an estimate of fault severity. Once all the datasets are stored in the learning stage, and the network is trained, then by giving the corresponding inputs to the network, the output of the network gives the value of number of broken bars.

Table 4.2 Test Results

Input A_1 (dB)	Input A_2 (dB)	Target Output	Actual Values	% error
-11.13	-10.55	0	0.0915	1
-11.35	-10.77	1	0.80876	19.12
-11.06	-10.46	2	0.98632	50.68
-10.93	-9.74	3	0.99103	66.94
			Average error	34.44

The Table 4.2 gives the test results. From the simulation results it is inferred that the percentage error is more.

CHAPTER 5
FUZZY LOGIC BASED FAULT DIAGNOSIS

5.1 INTRODUCTION

Problems in the real world quite often turn out to be complex owing to an element of uncertainty either in the parameters which define the problem or in the situations in which the problem occurs.

The uncertainty may arise due to partial information about the problem, or due to information which is not fully reliable, or due to inherent imprecision in the language with which the problem is defined, or due to receipt of information from more than one source about the problem which is conflicting. It is in such situations that fuzzy set theory exhibits immense potential for effective solving of the uncertainty in the problem. Fuzziness means 'vagueness'. Fuzzy set theory is an excellent mathematical tool to handle the uncertainty arising due to vagueness.

Fuzzy logic systems are universal function approximators. In general, the goal of the fuzzy logic system is to yield a set of outputs for given inputs in a non-linear system, without using any mathematical model, but by using linguistic rules. It has many advantages. They are

- Fuzzy logic is conceptually easy to understand. The mathematical concepts behind fuzzy reasoning are very simple. What makes fuzzy better is the "Naturalness" of its approach and not its far-reaching complexity.
- Fuzzy logic is flexible. With any given system, it's easy to massage it or layer more functionality on top of it without starting again from scratch.
- Fuzzy logic is tolerant of imprecise data. Everything is imprecise if you look closely enough, but more than that, most things are imprecise even on careful inspection. Fuzzy reasoning builds this understanding into the process rather than tacking it onto the end.
- Fuzzy logic can model nonlinear functions of arbitrary complexity. You can create a fuzzy system to match any set of input-output data. This process is made particularly easy by adaptive techniques like Adaptive Neuro-Fuzzy Inference Systems (ANFIS), which are available in the Fuzzy Logic Toolbox.
- Fuzzy logic can be built on top of the experience of experts. In direct contrast to neural networks, which take training data and generate opaque,

impenetrable models, fuzzy logic lets you rely on the experience of people who already understand your system.

- Fuzzy logic can be blended with conventional control techniques. Fuzzy systems don't necessarily replace conventional control methods. In many cases fuzzy systems augment them and simplify their implementation.
- Fuzzy logic is based on natural language. The basis for fuzzy logic is the basis for human communication. This observation underpins many of the other statements about fuzzy logic.

5.2 MAMDANI FUZZY LOGIC INFERENCE SYSTEM

Mamdani-type of fuzzy logic controller contains four main parts, two of which perform transformations. The four parts are

- Fuzzifier (transformation 1)
- Knowledge base
- Inference engine(fuzzy reasoning, decision-making logic)
- Defuzzifier(transformation 2)

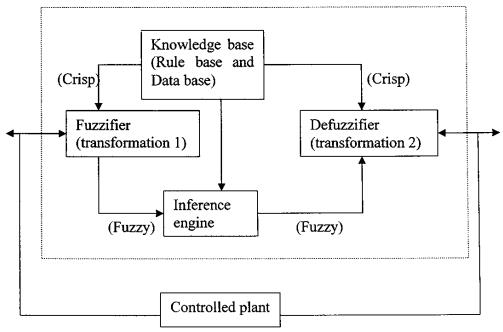

Figure 5.1 Mamdani Fuzzy Logic Inference Systems

5.2.1 Fuzzifier

The fuzzifier performs measurement of the input variables (input signals, real variables), scale mapping and fuzzification (transformation 1).thus all the monitoring input signals are scaled and fuzzification means that the measured signals (crisp input quantities which have numerical values) are transformed into fuzzy quantities. This transformation is performed by using membership functions. In a conventional fuzzy logic controller, the number of membership functions and the shapes of these are initially determined by the user. A membership function has a value between 0 and 1, and it indicates the degree of belongingness of a quantity to a fuzzy set. If it is absolutely certain that the quantity belongs to the fuzzy set, then its value is 1(it is 100% certain that the quantity belongs to this set), but if it is absolutely certain that it does not belong to this set then its value is 0. Similarly if for example the quantity belongs to the fuzzy set to an extent of 50%, then the membership function is 0.5.

There are many types of different membership functions, piecewise linear or continuous. Some of these are smooth membership functions, e.g. bell-shaped, sigmoid, Gaussian etc. and others are non-smooth, e.g. triangular, trapezoidal etc. the choice of the type of membership function used in a specific problem is not unique. Thus it is reasonable to specify parameterized membership functions, which can be fitted to a practical problem. If the number of elements in the universe X is very large or if a continuum is used for X then it is useful to have a parameterized membership function, where the parameters are adjusted according to the given problem. Parameterized membership functions play an important role in adaptive fuzzy systems, but are also useful for digital implementation. Due to their simple forms and high computational efficiency, simple membership functions, which contain straight line segments, are used extensively in various implementations. Obviously, the triangular membership function is a special case of the trapezoidal one.

Triangular membership function depends on three parameters a, b, c and can be described as follows by considering four regions.

$$\mu A'(x;a,b,c) = \begin{cases} 0 & x < a \\ (x-a)/(b-a) & a \le x \le b \\ (c-x)/(c-b) & b \le x \le c \\ 0 & x > c \end{cases} \qquad (4.1)$$

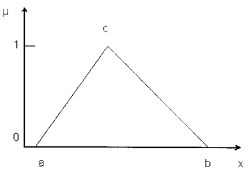

Figure 5.2 Triangular membership functions

A triangular membership function is shown in Figure 5.2 is used for both the input and output variable and the points a, b, c are also denoted. Alternatively, it is possible to give a more compact form

$$\mu^{A'}(x; a, b, c) = \max \{\min [(x-a) / (b-a), (c-x) / (c-b)], 0\} \qquad (4.2)$$

The detection of broken rotor bars fault severity is considered by utilizing Mamdani-style fuzzy inference and using as input variables the fault components A_1 and A_2 at frequencies $(1\pm 2s)f$. Small, Medium, Large are the three membership functions used for the input variable A_1 and A_2. Zero, One, Two, Three broken bar are the four membership functions used for the output variable number of broken bar.

5.2.2 Knowledge Base

The knowledge base consists of the data base and the linguistic control rule base. The data base provides the information which is used to define the linguistic control rules and the fuzzy data manipulation in the fuzzy logic controller. The rule base specifies the control goal actions by means of a set of linguistic control rules. In other words, the rule base contains rules such as would be provided by an expert. The fuzzy logic controller looks at the input signals and by using the expert rules determines the appropriate output signals (control actions). The rule base contains a set of if-then rules. The main methods of developing a rule base are:

- Using the experience and knowledge of an expert for the application and the control goals;
- Modeling the control action of the operator;
- Modeling the process;
- Using a self-organized fuzzy controller;
- Using artificial neural networks;

When the initial rules are obtained by using expert physical considerations, these can be formed by considering that the three main objectives to be achieved by the fuzzy logic controller are:

- Removal of any significant errors in the process output by suitable adjustment of the control output;
- Ensuring a smooth control action near the reference value (small oscillations in the process output are not transmitted to the control input);
- Preventing the process output exceeding user specified values;

By considering the two dimensional matrix of the input variables, each subspace is associated with a fuzzy output situation.

5.2.3 Inference Engine

It is the kernel of a fuzzy logic controller and has the capability both of simulating human decision–making based on fuzzy concepts and of inferring fuzzy control actions by using fuzzy implication and fuzzy logic rules of inference as shown in Figure 5.3. In other words, once all the monitored input variables are transformed into their respective linguistic variables, the inference engine evaluates the set of if-then rules and thus result is obtained which is again a linguistic value for the linguistic variable. This linguistic result has to be then transformed into a crisp output value of the fuzzy logic control.

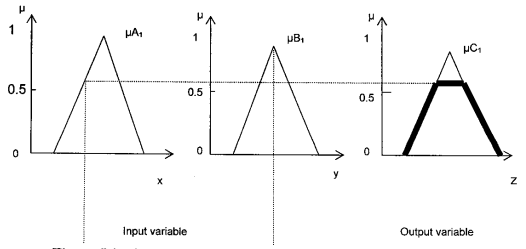

Figure 5.3 Graphical interpretation of fuzzification, inference

5.2.4 Defuzzifier

The second transformation is performed by the defuzzifier which performs scale mapping as well as defuzzification. The defuzzifier yields a non-fuzzy, crisp

control action from the inferred fuzzy control action by using the consequent membership functions of the rules. There are many defuzzification techniques. They are centre of gravity method, height method, mean of maxima method, first of maxima method, sum of maxima. In this project height method defuzzification technique is used as shown in Figure 5.4. In this method, the individual output membership functions for each rule are used (e.g. if for the fuzzy AND the min operator is used, then these are clipped membership functions) and first, the peak values (height), p_k, of the (clipped) consequent membership functions of all rules that have fired are multiplied by the ordinates of these membership functions(c_k). In a second step, these products are added and then divided by the sum of the peak values of the (clipped) consequent membership functions. It follows that the output value is

$$Z^{*H} = \frac{\sum p_k c_k}{\sum p_k} \qquad (4.3)$$

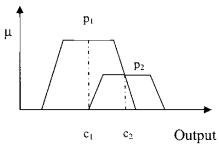

Figure 5.4 Height Defuzzification Method

5.3 FUZZY FAULT DIAGNOSIS

5.3.1 Offline Monitoring

5.3.1.1 Simulation of Fuzzy Fault Detector (FFD)

The fuzzy inference system used is Mamdani. Triangular membership function is used for both the input A_1 and A_2 and for the output. Three membership functions for the input variables and four memberships function for the output variable is selected.

Table 5.1 Fuzzy Rules

A_1 \ A_2	Small	Medium	Large
Small	Zero	Two	One
Medium	One	Two	Zero
Large	One	Three	Two

The Table 5.1 gives the nine fuzzy rules used in this project for offline condition monitoring. The simulated data suggest considering "small" to amplitude from -13.1 dB to -12.7 dB, "medium" from -12.9 dB to -12.3 dB, "large" from -12.4 dB to -12 dB for the input variable A1; "small" to amplitude from -33.23 dB to – 31.75 dB, "medium" from -32.06 dB to -30.2 dB, "large" from -30.5 dB to -28.9 dB for the input variable A2; "zero" to amplitude from -0.0953 to 0.782, "one" from 0.353 to 1.54,"two" from 1.08 to 2.25, "three" from 2.12 to 3.04 for the output variable broken bar; the amplitude of the fault components increases with the number of broken bars. The membership functions used for simulation are shown in Figures (Figure 5.5 – Figure 5.7). The Figure 5.8 shows the surface viewer of the FFD.

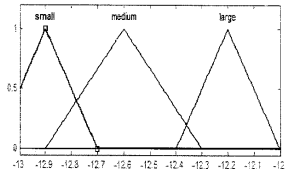

Figure 5.5 Input Membership Functions for A_1

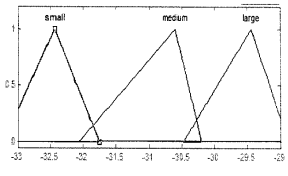

Figure 5.6 Input Membership Functions for A_2

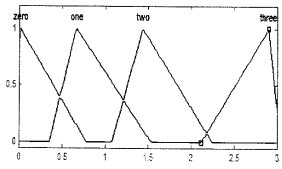

Figure 5.7 Output Membership Functions

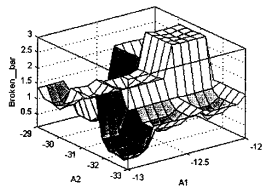

Figure 5.8 Surface Viewer

5.3.1.2 Simulation Results of FFD

The difference between the target and the actual is calculated for different inputs. The results obtained are shown in Table 5.2

Table 5.2 Simulation Results

Input A1 (Db)	Input A2 (Db)	Target Output	Actual Value	% error
-12.59	-29.55	0	0.09	1
-12.12	-32.49	1	0.99	1
-12.78	-31.65	2	2.01	0.5
-12.35	-30.91	3	3	0
			Average error	0.625

From the above table, it is inferred that the performance of fuzzy fault diagnosis system is comparable with conventional method.

5.3.2 Online Monitoring

5.3.2.1 Simulation of Fuzzy Fault Detector (FFD)

The fuzzy inference system used is Mamdani. Triangular membership function is used for both the input A_1 and A_2 and for the output. Three membership functions for the input variables and four memberships function for the output variable is selected.

Table 5.3 Fuzzy Rules

A_1 \ A_2	Small	Medium	Large
Small	One	One	Two
Medium	Zero	Two	Three
Large	Three	Two	Three

The Table 5.3 gives the nine fuzzy rules used in this project for online condition monitoring. The simulated data suggest considering "small" to amplitude from -11.5 dB to -11.3 dB, "medium" from -11.34 dB to -10.74 dB, "large" from -10.9 dB to -10.5dB for the input variable A1; "small" to amplitude from -10.9 dB to -10.5 dB, "medium" from -10.6 dB to -10 dB, "large" from -10.1 dB to -9.65 dB for the input variable A2; "zero" to amplitude from -0.6 to 0.218, "one" from 0.131 to 1.62,"two" from 1.36 to 2.33, "three" from 2.08 to 3.1 for the output variable broken bar; the amplitude of the fault components increases with the number of broken bars. The membership functions used for simulation are shown in Figures (Figure5.9 – Figure 5.11). The Figure 5.12 shows the surface viewer of the FFD.

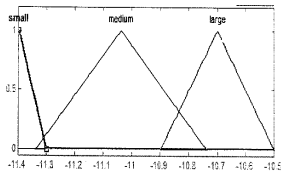

Figure 5.9 Input Membership Functions for A_1

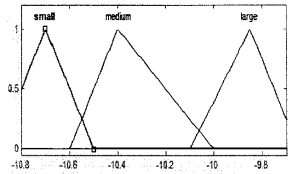

Figure 5.10 Input Membership Functions for A_2

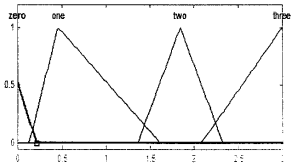

Figure 5.11 Output Membership Functions

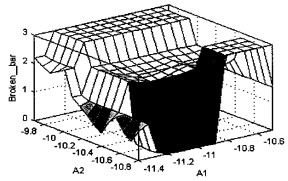

Figure 5.12 Surface Viewer

5.3.2.2 Simulation Results of FFD

The difference between the target and the actual is calculated for different inputs. The results obtained are shown in Table 5.4

Table 5.4 Simulation Results

Input A_1 (dB)	Input A_2 (dB)	Target Output	Actual Values	% error
-11.13	-10.55	0	0.09	1
-11.35	-10.77	1	1.02	2
-11.06	-10.46	2	1.98	1
-10.93	-9.74	3	3	0
			Average error	1

From the above table, it is inferred that the performance of fuzzy fault diagnosis system is comparable with conventional method.

5.4 COMPARISON OF NEURAL NETWORK AND FUZZY BASED FAULT DIAGNOSIS SYSTEM

Neural network approach is a black box approach, where the expert knowledge is hidden in the black box system in the form of weights and biases of the neural network. However, in fuzzy logic based system the actions of a human expert are clearly present in the rule base. Comparison of both the neural network and fuzzy based fault diagnoses for both the online and offline is given in Table 5.5.

Table 5.5 Comparison of Neural Network and Fuzzy Based Fault Diagnosis

% Error	Neural Network Diagnosis	Fuzzy Logic diagnosis
Off Line	29.4	0.625
On Line	34.44	1

From the above table, it is inferred that the fuzzy fault diagnosis gives reduced error compared with neural network based diagnosis.

CHAPTER 6

FUZZY OPTIMIZATION USING GENETIC ALGORITHM

6.1 INTRODUCTION TO GENETIC ALGORITHM

Genetic algorithm are good at taking larger, potentially huge, search spaces and navigating them looking for optimal combinations of things and solutions which we might not find in a life time.

Three most important aspects of using GA are:

- Definition of objective function
- Definition and implementation of genetic representation
- Definition and implementation of genetic operators.

During the creation of offspring, recombination occurs (due to cross over) and in that process genes from parents form a whole new chromosome in some way. The new created offspring can then be mutated. Mutation means that the element of DNA is modified. These changes are mainly caused by errors in copying genes from parents. The fitness of an organism is measured by means of success of organism in life.

GA's is usually suitable for solving maximization problems. Minimization problems are usually transformed into maximization problems by some suitable transformation. In general, fitness function F(X) is first derived from the objective function and used in successive genetic operations. Here error is used as the fitness function and the objective function is to minimize the error.

A simple genetic algorithm genetic algorithm largely uses three basic operators which are

- Reproduction
- Cross over
- Mutation.

6.1.1 Reproduction

Reproduction is usually the first operator applied on population. Chromosomes are selected from the population to the parents to cross over and produce offspring. According to Darwin's evolution theory of survival of the fittest, the best ones should survive and create new offspring. There exist a number of reproduction operators in GA literature but the essential idea in all or them is that the

above average strings are picked from the current population and their multiple copies are inserted in the mating pool in a probabilistic manner. The various methods of selecting chromosomes for parents to cross over are:

- Roulette-wheel selection
- Boltzmann selection
- Tournament selection
- Rank selection
- Steady-state selection

Roulette-wheel selection is used in this project. The commonly used reproduction operator is the proportionate reproductive operator where a string is selected from the mating pool with a probability proportional to the fitness.

6.1.2 Cross over

After the reproduction phase is over, the population is enriched with better individuals. Reproduction makes clones of good strings, but does not create new ones. Cross over operator is applied to the mating pool with a hope that is would create a better string. The aim of the cross over operator is to search the parameter space. In addition, search is to be made in a way that the information stored in the present string is maximally preserved because these parent strings are instances of good strings selected during reproduction.

Cross over is a recombination operator, which proceeds in there steps. First, the reproduction operator selects at random a pair of two individual strings for mating, then a cross-site is selected at random along the string length and the position values are swapped between two strings following the cross site. For instance, let the two selected strings in a mating pair be A = 11**111** and B = 00**000**. If the random selection of a cross-site is two, then the new strings following cross over would be A*=11**000** and B*=00**111**.This is a single-site cross over. Though these operators look very simple, their combined action is responsible for much of GA's power. From a computer implementation point of view, they involve only random number of generations, string copying, and partial string swapping. There exist many types of cross over operations in genetic algorithm.

- Single-site Cross Over - Single site is chosen for cross over.
- Two-point Cross Over - Two-point is chosen for cross over.
- Multi-point Cross Over - Multi-point is chosen for cross over.

6.1.3 Mutation operator

After crossover, the strings are subjected to mutation. Mutation of a bit involves flipping it, changing 0 to 1 and vice versa. The bit-wise mutation is performed bit-by-bit. If the mutation at that site is selected flipping is true, otherwise the outcome is false. If at any bit, the outcome is true then the bit is altered, otherwise the bit is kept unchanged.

For example, consider the following population having four eight-bit strings.

0110 1011
0011 1101
0001 0110
0111 1100

Notice that all four strings have a zero in the leftmost bit position. If the true optimum solution requires a one in that position, then neither reproduction nor cross over operator described above will be able to create one in that position.

0110 1011
0011 1101
0001 0110
1111 1100

6.2 MEMBERSHIP FUNCTION OPTIMIZATION

6.2.1 Tuning Membership Function

In a fuzzy logic system it is possible to obtain final (tuned) membership functions by using genetic algorithms. For this purpose initial membership functions for the various fuzzy variables are assumed, given some functional mapping of the system. Parameters of the initial membership functions are then generated and coded as bit strings that are then concatenated to make one long string to represent the whole parameter set of the membership functions. A fitness function is then used to evaluate the fitness value of each set of membership functions (parameters that define the functional mapping of the system). Then the reproduction, crossover and mutation operators are applied as to obtain the optimal population (membership functions), or more precisely, the final tuned value of the parameter set describing the membership functions used. The Figure 6.1 shows the input variable for the optimization.

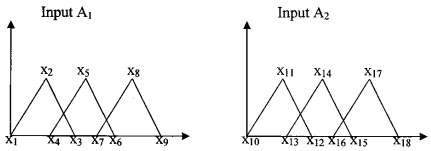

Figure 6.1 Membership Function of Input A_1 and A_2.

It is assumed that the system under consideration has known crisp input-output data. After the initial population is obtained, it is possible to compute for all the crisp inputs the corresponding crisp output data by using fuzzy rules shown in Table 5.3 together with the membership functions corresponding to the initial population. To be more precise, the first binary string obtained randomly, contains a parameter set of the membership functions used, and these membership function together with the input data yield output values. But these will not necessarily equal to the crisp values in the output data, since the initially used membership functions are not correct, and thus output errors exist. The output errors are used to obtain a fitness value of the string.

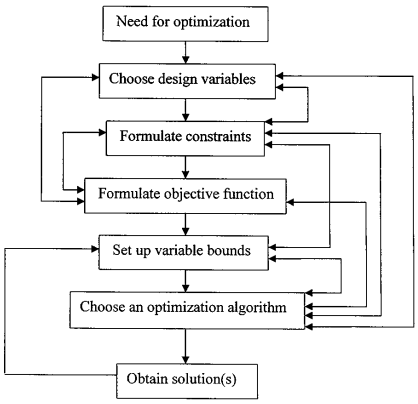

Figure 6.2 Flowchart of the Optimal Design Procedure

The objective function is to minimize the error. Reproduction is done by generating a random number between 0 and 1 and its occurrence is checked in the population and that particular string is selected. Single point crossover is used. The site is selected randomly. The bit is selected randomly for mutation and flipping it, changing 0 to 1 and vice versa. Figure 6.2 shows an outline of the steps involved in an optimal design formulation process.

6.2.2 Algorithm

The objective function is to minimize the error and the steps involved are as follows.

Step 1 : Get the population size, number of substring, number of gene in a chromosome.

Step 2 : Get the upper and lower bound values.

Step 3 : Generate the binary bits and calculate its decimal value.

Step 4 : Calculate the x_i value using the formula given.

$$x = x_L * (x_U - x_L) / (2^L - 1) * \text{Decimal value} \quad (5.1)$$

Step 5 : Calculate the fitness function f(x), if termination criteria is satisfied, terminate.

$$f(x) = \text{target} - \text{actual} \quad (5.2)$$

Step 6 : Calculate f'(x), A_i, B_i, C_i.

$$f'(x) = 1/(1+f(x)) \quad (5.3)$$

$$A_i = f'(x) / \text{average } f'(x) \quad (5.4)$$

$$B_i = A_i / \sum A \quad (5.5)$$

$$C_i = B_1 + B_2 + \ldots\ldots B_i \quad (5.6)$$

Step 7 : Generate random numbers as D and the best chromosome is created.

Step 8 : Select the swapping pair for crossover, bit for the mutation and the new population is created.

6.3 SIMULATION RESULTS

Number of variable (substring) = 18 (x_1 to x_{18})
Population size = 5
Number of gene in a chromosome = 5

Table 6.1 Fuzzy Optimization Using Genetic Algorithm

A_1	Small			Medium			Large		
Population	X1	X2	X3	X4	X5	X6	X7	X8	X9
1	-11.508064	-11.424193	-11.304839	-11.315806	-11.011613	-10.757742	-10.914516	-10.662903	-10.485484
2	-11.479033	-11.35	-11.346774	-11.312581	-11.005807	-10.702903	-10.946774	-10.717742	-10.485484
3	-11.491936	-11.420968	-11.311291	-11.315806	-11.014516	-10.706129	-10.917742	-10.672581	-10.498387
4	**-11.479033**	**-11.375807**	**-11.346774**	**-11.306129**	**-11.005807**	**-10702903**	**-10.920968**	**-10.717742**	**-10.479033**
5	-11.491936	-11.420968	-11.324194	-11.315806	-11011613	-10.706129	-10.917742	-10.659678	-10.498387

Table 6.2 Fuzzy Optimization Using Genetic Algorithm

A_2	Small			Medium			Large			Error
Population	X10	X11	X12	X13	X14	X15	X16	X17	X18	
1	-10.853226	-10.662903	-10.517742	-10.617742	-10.385484	-9.982258	-10.05	-9.877419	-9.696774	0.20001
2	-10.943548	-10.714516	-10.508064	-10.643548	-10.391935	-9.956451	-10.019032	-9.870968	-9.609677	0.199995
3	-10.853226	-10.714516	-10.514516	-10.624193	-10.42742	-9.988709	-10.044193	-9.880645	-9.687097	0.200005
4	**-10.943548**	**-10.714516**	**-10.533871**	**-10.643548**	**-10.398387**	**-9.956451**	**-10.019032**	**-9.896774**	**-9.609677**	**0.19999**
5	-10.85	-10.714516	-10.514516	-10.61129	-10.42742	-9.991936	-10.044193	-9.880645	-9.7	0.2

Table 6.3 Comparison of Conventional and Optimized Method

Techniques	Input	Small			Medium			Large			% error
		x_1	x_2	x_3	x_4	x_5	x_6	x_7	x_8	x_9	
conventional	A_1	-11.5	-11.4	-11.3	-11.34	-11.04	-10.74	-10.9	-10.7	-10.5	Conventional 1
optimized		-11.479033	-11.375807	-11.346774	-11.306129	-11.005807	-10702903	-10.920968	-10.717742	-10.479033	
Techniques		x_{10}	x_{11}	x_{12}	x_{13}	x_{14}	x_{15}	x_{16}	x_{17}	x_{18}	
conventional	A_2	-10.9	-10.7	-10.5	-10.6	-10.4	-10	-10.1	-9.85	-9.65	Optimized 0.1999
optimized		-10.943548	-10.714516	-10.533871	-10.643548	-10.398387	-9.956451	-10.019032	-9.896774	-9.609677	

From the number of chromosomes generated, the best fit is selected by choosing the lowest error in the Tables (Table 6.1 and 6.2). The fourth chromosome gives the best result of 0.1999 percentage of error. Comparison of the fuzzy approach using conventional method and optimization technique using genetic algorithm for fault detection is shown in Table 6.3. From the table it is inferred that the error percentage compared with the conventional technique is reduced in optimization technique using genetic algorithm.

CHAPTER 7
CONCLUSION AND FUTURE SCOPE

The rotor fault detection methods for three phase induction motor have been implemented using neural network and fuzzy logic. The technique is based on monitoring the stator current spectrum. In this project faults under various broken bar condition are monitored and the results are presented. The sidebands at (1± 2s)f are taken as the inputs for neural network and fuzzy logic fault detector The parameter in neural and fuzzy fault detection is compared in terms of percentage of error. From the simulation results, it is inferred that the fuzzy logic based fault diagnosis gives the reduced percentage error than the neural network based fault diagnosis. Hence fuzzy logic based fault diagnosis is the effective method for fault detection. The membership function is tuned using genetic algorithm. From the simulation results, it is inferred that this technique gives reduced error compared with the conventional tuning.

Further works that can be implemented in this project are,

- The fault detection scheme can be carried out using neuro-fuzzy techniques.
- This scheme can also be extended to other types of motors.
- Rules can be optimized using genetic algorithm.
- Neural weights can also be optimized using genetic algorithm.

REFERENCES

1. Laurene Fausett (2004), 'Fundamentals of Neural Networks', *Pearson Education Pte. Ltd., Delhi.*

2. Peter Vas (1993), 'Parameter Estimation, Condition Monitoring and Diagnosis of Electrical Machines', *Clarendron Press, Oxford.*

3. Peter Vas (1999), 'Artificial Intelligence-Based Electrical Machines and Drives', *Oxford University.*

4. Kalyonmoy Deb, 'Optimization for Engineering Design: Algorithm and Examples', *Prentice Hall of India Pvt. Ltd.*

5. Rajasekaran.S and Vijayalakshmi Pai.G.A (2005) 'Neural Networks, Fuzzy Logic and Genetic Algorithm Synthesis and Applications', *Prentice Hall of India Pvt. Ltd.*

6. Jafar Milimonfared, Honayoun Meshgin Kelk and Subhasis Nandi, (1999), 'A Novel Approach for Broken- Rotor – Bar Detection in Cage Induction Motor', *IEEE Transaction-Industry Application, Vol 35, No. 5, Pp 1000 – 1005.*

7. Mohamed Ei Hacheni Benbouzid and Gerald B.Kliman, (2003), 'What Stator Current Processing Based Techniques to use for Induction Motor Fault Diagnosis?', *IEEE Transaction-Energy Conversion, Vol 18, No. 2, Pp 238 – 244.*

8. Filippetti. F, Franceschini.G and Tassoni.C (1995), 'Neural Networks Aided On Line Diagnolistic of Induction Motor Faults', *IEEE Transaction – Industry Application, Vol 31 , No 4, Pp 316 – 323.*

9. Filippetti.F, Franceschini.G, Tassoni.C and Peter Vas(1998),'Recent Development of Induction Motor Drive Fault Diagnosis using AI Techniques', *IEEE Transaction – Industry Application, Vol 34, No 4,Pp 1966 – 1973.*

10. Filippetti.F, Franceschini.G, Tassoni.C and Peter Vas (1996), 'AI Techniques in Induction Machines Diagnosis Including the Speed Ripple Effect', *IEEE IAS Annual Meeting Conference, San Diego, Pp 655-662.*

11. Sinan Altug, Mo- Yuen Chow and II Joel Trusell (1999), 'Fuzzy Inference Systems Implemented on Neural Architectures for Motor Fault Detection and Diagnosis', *IEEE Transaction – Industrial Electronics, Vol 46, No 6, Pp 1069 - 1079.*

12. Yi – Sheng Zhou and Lin – Ying Lai (2000), 'Optimal Design for Fuzzy Controllers by Genetic Algorithm', *IEEE Transaction – Industry Application, Vol 36, No 1, Pp 93-97.*

13. Filippetti.F, Franceschini.G, Tassoni.C and Peter Vas (1994), 'Broken Bar Detection in Induction Machines: Comparison between Current Spectrum Approach and Parameter Estimation Approach', *Proceedings of the IEEE IAS Annual Meeting Conference, Vol 1, Pp 95 -102.*

14. Homayoun Meshgin – Kelk, Jafar Milimonfared and Hamid Toyilat (2004), 'Interbar Currents and Axial Fluxes in Healthy and Faulty Induction Motors', *IEEE Transaction – Industry Application, Vol 40, No 1, Pp 128-134.*

15. Mohamed EI Hacheni Benbouzid (2000), 'A Review of Induction Motor Signature Analysis as a Medium for Fault Detection', *IEEE Transaction – Industry Electronics, Vol 47, No 5, Pp 128-134.*